AEROSPACE REPORT NO.
ATR-80(7813)-1

The Distribution of Maximum Temperatures of Coronal Active Region Loops

Prepared by

E. B. MAYFIELD
Space Sciences Laboratory
The Aerospace Corporation
and
R. G. TESKE
Astronomy Department
University of Michigan, Ann Arbor

15 May 1980

Prepared for

NATIONAL AERONAUTICS AND SPACE ADMINISTRATION
Marshall Space Flight Center, Huntsville, Ala. 35812

Contract No. NAS 8-33112

Laboratory Operations
THE AEROSPACE CORPORATION

Aerospace Report No.
ATR-80(7813)-1

THE DISTRIBUTION OF MAXIMUM TEMPERATURES OF CORONAL ACTIVE REGION LOOPS

Prepared by

E. B. Mayfield
Space Sciences Laboratory
and
R. G. Teske
Astronomy Department
University of Michigan, Ann Arbor

15 May 1980

Laboratory Operations
THE AEROSPACE CORPORATION
El Segundo, Calif. 90245

Prepared for

NATIONAL AERONAUTICS AND SPACE ADMINISTRATION
Marshall Space Flight Center, Huntsville, Ala. 35812

Contract No. NAS 8-33112

Page intentionally left blank

Aerospace Report No.
ATR-80(7813)-1

THE DISTRIBUTION OF MAXIMUM TEMPERATURES OF CORONAL ACTIVE REGION LOOPS

Prepared

E. B. Mayfield

E. B. Mayfield

R. G. Teske per EBM

R. G. Teske

Approved

G. A. Paulikas

G. A. Paulikas, Director
Space Sciences Laboratory

Page intentionally left blank

ABSTRACT

Starting with the integrated emission measure distributions Q(T) of solar active regions, we determine the distribution of the parameter T_{max} which characterises individual plasma loops. The observed Q(T) were determined by combining EUV and X-ray data from two separate experiments on ATM/Skylab.

Page intentionally left blank

CONTENTS

Page intentionally left blank

FIGURES

Page intentionally left blank

TABLES

I. INTRODUCTION

The structure of the "closed" solar corona has received much attention recently. Following the realization that coronal active regions consist of an ensemble of plasma loops (c.f. Vaiana et. al., 1976), great progress has been made in modelling stable, quiescent loops under assumptions regarding the local energy balance (Rosner, Tucker and Vaiana, 1978; Craig, McClymont and Underwood, 1978; Emslie and Machado, 1978; Vesecky, Antiochos and Underwood, 1979; Levine and Pye, 1979). Conclusions drawn by the various investigators, (c.f. Pye, et al., 1978) are that in stable loops the role of mass flow is negligible and that the process of non-thermal energy deposition is directly balanced by radiative losses; thermal conduction along a loop is simply the means by which heat is redistributed from one place to another.

In papers cited above, successful comparison of predictions of the models with values of pressure, loop length, and maximum temperature inferred from observations, have given confidence that energy-balance models are appropriate and useful descriptions of physical processes in active regions. These models are all very similar to one another. Antiochos (1979) and Habbal and Rosner (1979) have explored the conditions under which coronal plasma loops are stable; their work places limits upon the chromospheric heat flux that is required for stability (Antiochos, 1979) and upon the nature of the non-thermal energy supply mechanism (Habbal and Rosner, 1979).

Given that loop stability is physically realizable and that the loops may be modelled on basis of local energy equilibrium, it remains to describe

the distribution of loops in an active region. Although instrumentation is available to provide resolved images of loops (c.f. Foukal, 1976) the nested loops of active regions are generally not resolved from one another. It is therefore essential that methods be developed by which the integrated properties of active regions may be made to yield information about the distribution of properties of individual loops. Levine and Pye (1979) have undertaken to do this; their method, based upon observational determination of the emission measure distribution for an active region, revealed some of the limitations of an emission measure analysis as it might be applied to this problem.

We have carried out a similar analysis of several coronal active regions, and have derived the emission measure distribution for them by combining EUV line fluxes with broad-band X-ray fluxes to achieve a picture of Q(T) across the range $4.5 < \log T < 6.5$. With these emission measure distributions we are able to determine the distributions of a simple loop parameter - the maximum temperature T_m - starting with simple numerical loop models. The present paper describes this work, which we think holds promise for future development.

II. SELECTION AND TREATMENT OF OBSERVATIONS

Our aim, like that of Levine and Pye (1979), is to develop a method by which the physical properties of individual plasma loops may be determined in unresolved active regions by an analysis of the emission measure distribution Q(T), which is defined by

$$Q(T)\ dT = N_e^2 dV. \qquad (1)$$

To obtain information about Q(T) across a wide range of temperature we have used ATM/Skylab data, and have combined broad-band X-ray images from the Aerospace/MSFC S-056 telescope with EUV raster scans obtained by the HCO S-055 spectroheliometer.

a. Selection of Active Regions

Three small, non-flaring active regions were studied. All were only a few days old when observed. Because they were essentially free of reported flaring, the derived description of the active region should refer only to quiescent, stable loops. Details of the observations are listed in Table I.

b. X-Ray Observations

We have used X-ray images photographed through two filters in the S-056 telescope: Filter 1 (12.7 μm Al, band-pass 8-16A) and Filter 2 (6.35 μ Al, band-pass 8-22A). Details of the instrument are discussed by Underwood et al., (1977). The calibrations and techniques of analysis are described by Underwood and McKenzie (1977).

From the latter we directly adopted $\mathcal{F}_j(T)$, the solar spectral flux at the telescope focal plane per unit emission measure on the sun, for the j-th filter. Curves of $\mathcal{F}_j(T)$ for j = 1, 2 are shown in our Figure 1.

Copies of the flight film were microdensitometered with a 1.4 arcsec^2 aperture and the photographic densities transformed via photometric calibration to F_j, the number of deposited photons/cm^2 of flight film. For a single pixel,

TABLE I

OBSERVED AND CALCULATED EUV AND X-RAY FLUXES

McMath Plage	Date 1973	Time of Observation, UT EUV	Time of Observation, UT X-Ray		Fluxes CIII λ977	Fluxes OVI λ1032	Fluxes MgX λ625	Fluxes X-Ray #1	Fluxes X-Ray #2
12364	30 May	1536	1710	Observed:	2.671(24)	1.237(24)	3.047(23)	6.920(4)	5.170(5)
				Calculated:	2.675(24)	1.238(24)	3.049(23)	6.893(4)	5.203(5)
12364	31 May	1946	1645	Observed:	1.671(24)	2.921(24)	2.758(23)	2.970(4)	2.380(5)
				Calculated:	1.670(24)	2.920(24)	2.763(23)	3.001(4)	2.350(5)
12375	6 June	2029	1418	Observed:	1.166(24)	2.174(24)	2.304(23)	1.870(4)	1.480(5)
				Calculated:	1.162(24)	2.171(24)	2.302(23)	1.868(4)	1.478(5)
12378	8 June	0214	0201	Observed:	1.170(24)	2.000(24)	2.598(23)	0.979(4)	0.776(5)
				Calculated:	1.170(24)	2.000(24)	2.586(23)	0.969(4)	0.786(5)
12378	8 June	1423	1607	Observed:	1.300(24)	2.429(24)	3.071(23)	0.995(4)	0.841(5)
				Calculated:	1.296(24)	2.426(24)	3.079(23)	0.999(4)	0.836(5)
12378	8 June	1429	1607	Observed:	1.430(24)	2.714(24)	3.215(23)	0.995(4)	0.841(5)
				Calculated:	1.426(24)	2.711(24)	3.222(23)	0.998(4)	0.837(5)
12378	8 June	1620	1607	Observed:	1.448(24)	2.880(24)	3.198(23)	0.995(4)	0.841(5)
				Calculated:	1.444(24)	2.877(24)	3.205(23)	0.998(4)	0.837(5)
12378	9 June	0138	1342	Observed:	1.121(24)	2.225(24)	2.722(23)	0.853(4)	0.826(5)
				Calculated:	1.121(24)	2.224(24)	2.743(23)	0.874(4)	0.802(5)

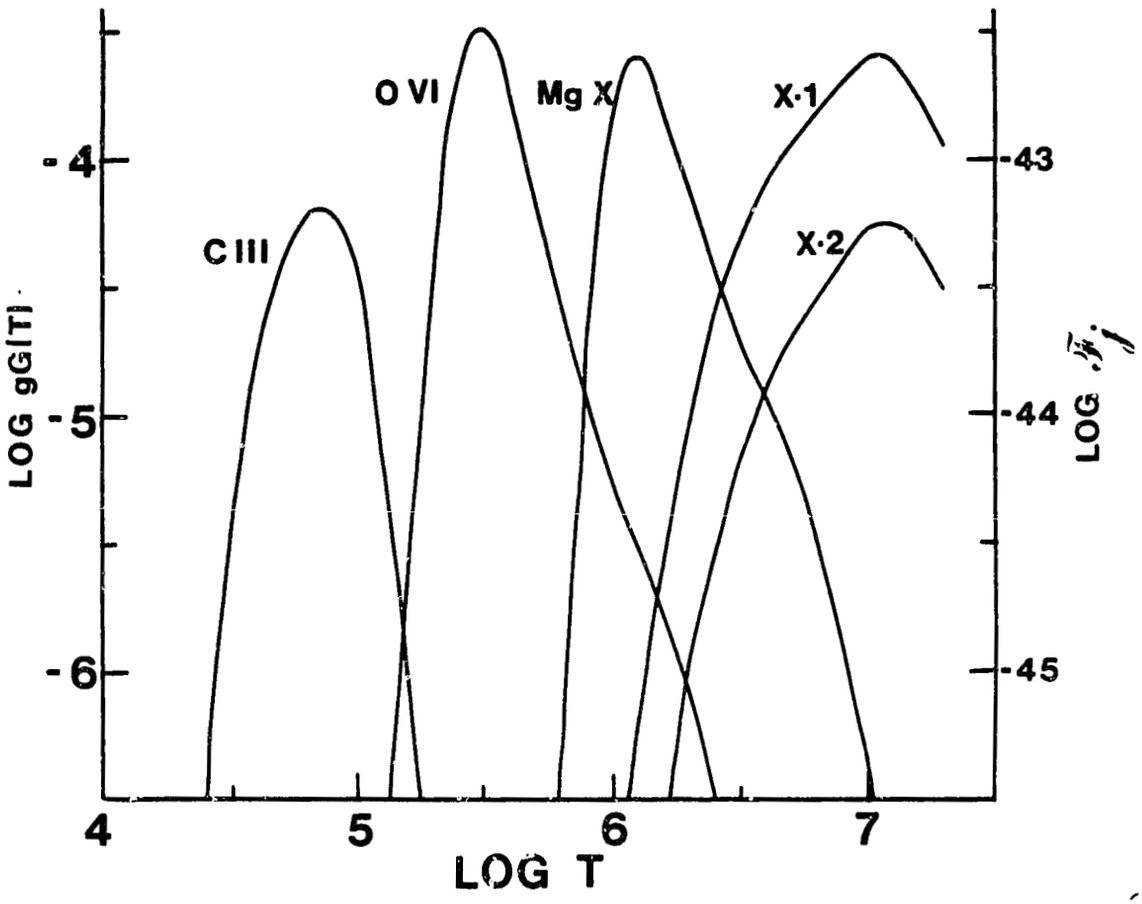

Figure 1. Values of log gG(T) for the Three EUV Lines That Were Used in this Study (Given by the Left-Hand Scale) and Values of Log $\mathcal{F}_j$ for the Two X-Ray Bands Used in the Study (Given by the Right-Hand Scale).

$$\frac{F_j}{t} = \frac{A}{a}\int \mathcal{F}_j(T)\ N_e^2 dV, \qquad (2)$$

where t = exposure time, A = telescope aperture, a = pixel area. Using the definition of Q(T), the full image of an active region yields the flux in photons sec^{-1}:

$$\int \frac{F_j}{t}\, dx dy = \frac{A}{a}\int \mathcal{F}_j(T)\ Q(T)\ dT \qquad (3)$$

In practice there was a slight background fog; we subtracted this background from the calculated X-ray flux to obtain corrected estimates. No account was taken of vignetting in the telescope.

c. EUV Observations

EUV rasters used by us were made in the first grating position of the S-055 spectroheliometer (Reeves, Huber and Timothy, 1977). We used data from CIII λ977, OVI λ1032, MgX λ625. Calibrations are given by Reeves, Timothy, Huber and Withbroe (1977).

The line fluxes in ergs sec^{-1} are (Withbroe, 1975):

$$I_\lambda = 4\pi \cdot 1.73 \times 10^{-16} A_{el}\ f\ g_{eff} \int G(T)\ Q(T) dT. \qquad (4)$$

Atomic parameters and abundances that we adopted are given in Table II together with the calibration factor that converts the measured count rate (N counts/0.041 sec) to fluxes I_λ.

Ionization equilibrium for Be-like CIII and Li-like OVI and MgX is sensitive to electron density (Vernazza and Raymond, 1979). In our work we used their ionization equilibrium calculations for an adopted $p_o = 1. \times 10^{16}$ K cm^{-3}, a value based upon the results of Nicolas et al. (1979), who obtained

TABLE II

DATA FOR CALCULATION OF EUV FLUXES

Line	A_{el}	f	g_{eff}	Calibration Factor
C III λ977	3.8×10^{-4}	0.14	0.60	1.55
O VI λ1032	2.1×10^{-4}	0.13	0.92	1.73
Mg X λ625	3.2×10^{-5}	0.041	1.2	1.48

$4.6 \times 10^{15} \lesssim p_o \lesssim 1.8 \times 10^{16}$ K cm^{-3} from Si III ratios in active regions observed with high spatial resolution. Their data may accurately reflect conditions at foot-points of individual loops. Vernazza and Raymond (1979) derived values of $10^{11} \lesssim N_e \lesssim 2 \times 10^{11}$ cm^{-3} in active regions, suggesting p_o-values somewhat higher than those used here; their result is however derived from spectra (Vernazza and Reeves, 1977) of a more energetic active region than the ones we have examined.

A difficulty posed by inclusion of CIII λ977 in this analysis is non-equilibrium ionization associated with vertical mass motions through the transition region (Raymond and Dupree, 1978). Upflows can increase the line's intensity by as much as 30%; downflows, which are commonly seen (Raymond and Dupree, 1978; Nicolas et al., 1979) can decrease its intensity by a factor of up to 5.

In CIII a significant population of ions is in the low-lying metastable ^3P state and in other excited states (Dupree, 1972), so that it is necessary to introduce a correction factor into equation (4) to account for underpopulation of the ground state. The factor, varying from unity at low temperatures to ~ 0.3 at log T = 4.5 and higher (for $p_o = 10^{16}$ K cm^{-3}), has been incorporated in our calculations.

Values of g_{eff} G(T) for each ion are plotted in Fig. 1; these include the excitation factor for CIII λ977.

Observed fluxes were integrated within a rectangular area on the raster scans that included the selected active regions and a small portion of their surroundings. The ratios of line brightness (active/quiet) is large enough (Dupree et al., 1973; Vernazza and Reeves, 1977) that no great error is made

by this procedure. Indeed we found that reasonable variations of integration boundaries changed the measured EUV fluxes by at most five percent. Our solutions for Q(T) are stable against greater data fluctuations than that (see below).

III. CALCULATION OF EMISSION MEASURES

Emission measure distributions Q(T) were calculated using Withbroe's (1975) iterative method. Table I lists the observed fluxes and the fluxes calculated from the (converged) Q(T) - distributions. We considered a solution to be converged when the trial Q(T) had changed by less than 0.5% at all temperatures between iterations. While the final Q(T) do not reproduce the input fluxes perfectly, the agreement between input fluxes and calculated fluxes in most cases is within 1%, except for the June 9 data, for which the Q(T) solution remained unconverged after 75 iterations.

Graphs of our Q(T) are shown in Figure 2.

We tested the stability of the method, as applied by us, by randomly perturbing one set of input data (Dere, 1978; Levine and Pye, 1979). With a random number generator we varied the input fluxes by up to 10% of their initial value; the Q(T) determined from the disturbed data were allowed to converge without limiting the number of iterations. Table III lists the means and standard deviations that resulted from 23 computer runs, and shows that our Q(T) are surprisingly stable against data errors.

Our June 9 results are not secure, for two reasons: (i) a part of the region fell outside the raster area, and we had to estimate corrections for that; (ii) the EUV and X-ray observations were made 12 hours apart. This is

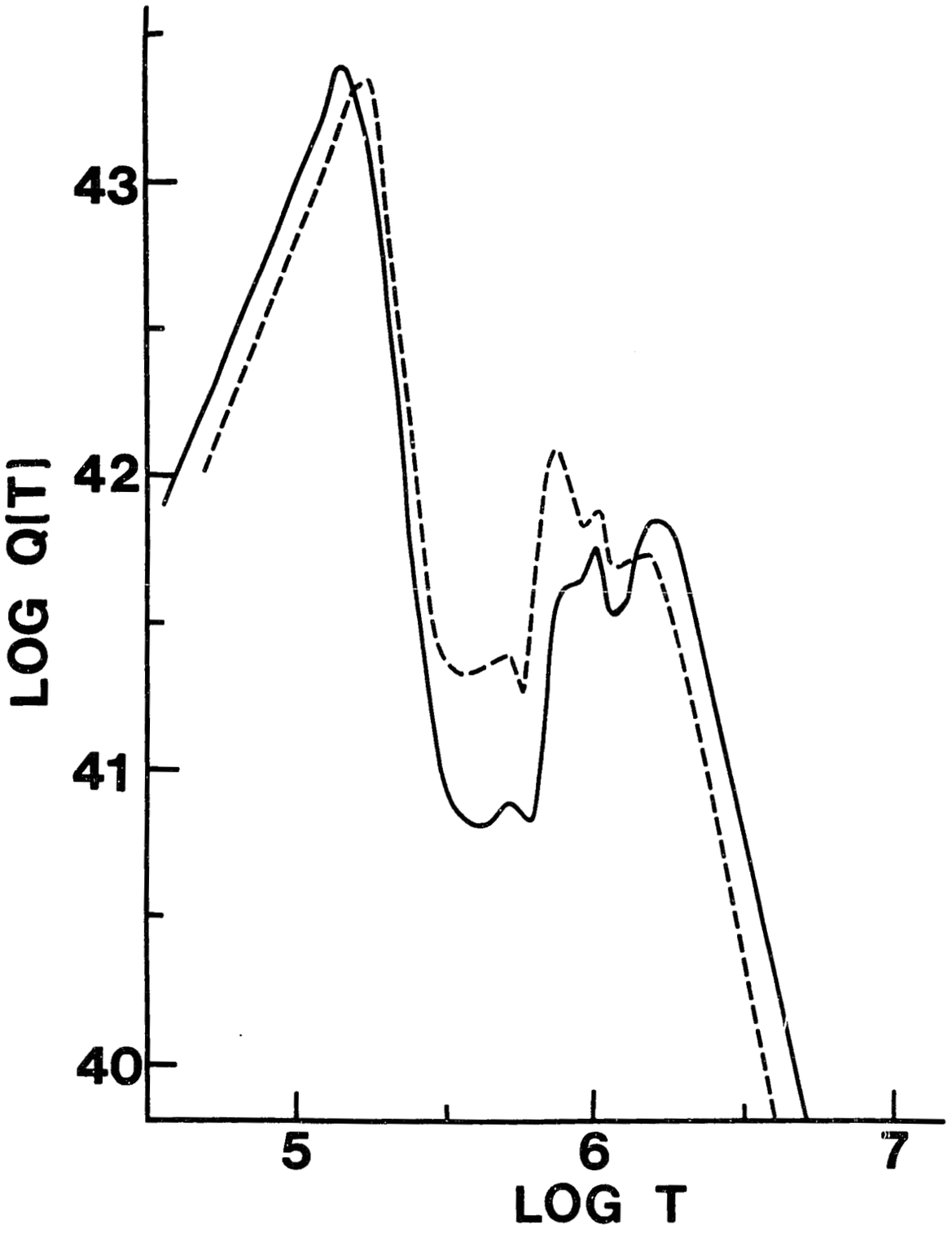

Figure 2(a). Emission Measures Q(T) for the Coronal Active Regions. Region 12364 at 1536 UT on 30 May 1973 (solid curve) and at 1946 UT on 31 May 1973 (dashed curve).

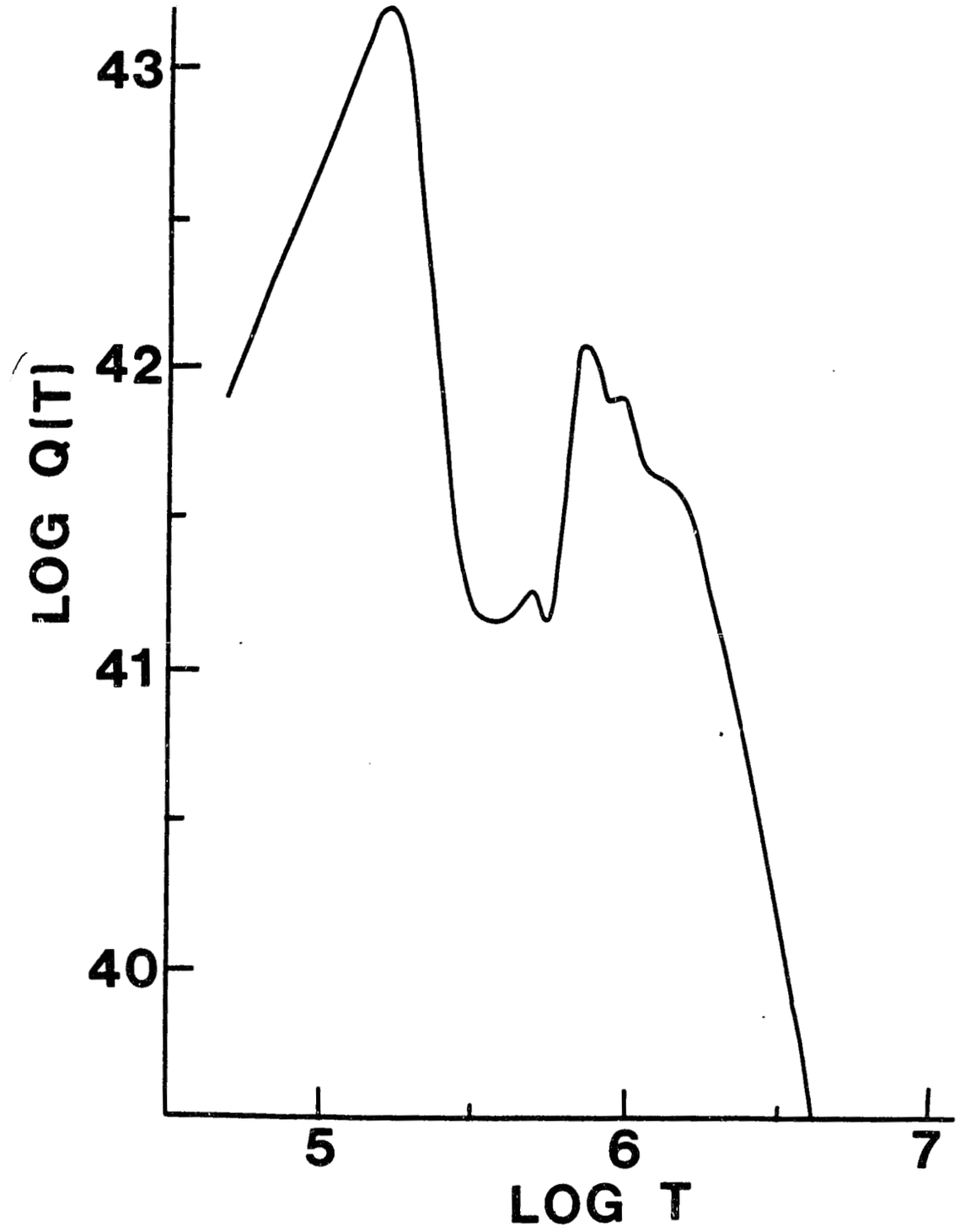

Figure 2(b). Emission Measures Q(T) for the Coronal Active Regions. Region 12375 at 2029 UT on 6 June 1973.

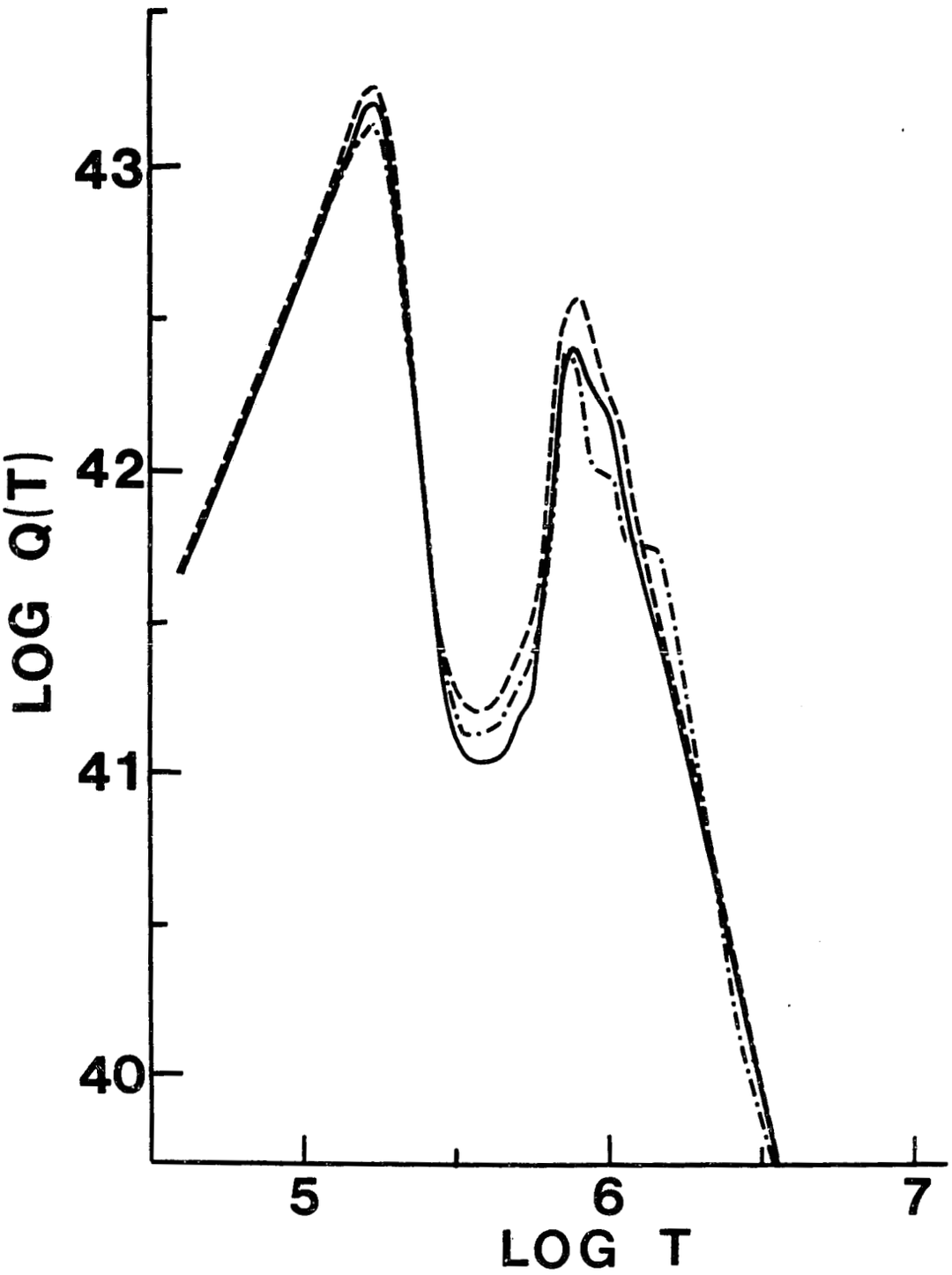

Figure 2(c). Emission Measures Q(T) for the Coronal Active Regions. Region at 0214 UT on 8 June 1973 (solid curve), at 1620 UT on 8 June 1973 (dashed curve), and at 0138 UT on 9 June 1973 (dot-dash curve).

TABLE III

STANDARD DEVIATIONS OF Q(T) AND w_m (T_m)

RANDOMLY PERTURBED DATA 0214 UT

JUNE 8, 1973

log T	<Q(T)>	$\sigma_{Q(T)}$	<w_m (T_m)>	σ_{w_m}
4.6	4.36 (41) $cm^{-3}K^{-1}$	2.56 (40) $cm^{-3}K^{-1}$	-	-
4.8	1.38 (42)	8.09 (40)	-	-
5.0	4.36 (42)	2.56 (41)	-	-
5.2	1.31 (43)	7.72 (41)	-	-
5.4	5.34 (41)	4.03 (40)	-	-
5.6	1.09 (41)	1.09 (40)	10.1	2.6
5.8	6.87 (41)	9.04 (40)	27.4	4.1
6.0	1.62 (42)	3.54 (41)	14.2	3.1
6.2	1.85 (41)	7.11 (40)	0.32	0.12
6.4	2.12 (40)	3.51 (39)	0.0074	0.0012
6.6	2.48 (39)	4.80 (38)	-	-
6.8	2.75 (38)	9.83 (37)	-	-
7.0	3.33 (37)	2.09 (37)	-	-

probably why the solution for Q(T) did not readily converge.

Our Q(T) distributions in Figure 2 show corrugations in the temperature range $5.7 < \log T < 6.2$ that are probably artefacts of the iterative fitting process (Withbroe, 1975). The log T - locations of the dips correspond closely with regions of overlap of the log g G(T) and log F_j curves of Figure 1, and likely reflect an incompatability between the EUV and X-ray calibrations or in the atomic data. For example, the oxygen abundance adopted by Underwood and McKenzie (1977) in their F_j - calculations is a factor 3.5 lower than the abundance adopted by us.

Over the range $\log T > 5.8$ our Q(T) distributions are in reasonable agreement with the results derived by Withbroe (1975; 1977) and by Levine and Pye (1979), except that the maxima in our Q(T) tend to lie at lower temperatures then theirs. Whether this is due to the combination of EUV lines and X-ray bands used by us, or is an intrinsic property of such small quiescent regions cannot be stated. We note, however, that reported subflaring occurred only in region 12364, observed by us on May 30; Q(T) for this region has its maximum at a higher temperature than in our other distributions, in excellent accord with Withbroe, and Levine and Pye.

Below $\log T < 5.5$, our calculations show a rising Q(T) corresponding to plasma below the transition zone. Withbroe's (1977) empirical emission measure distribution also showed an upper chromospheric rise of Q(T), but at lower temperatures than those obtained by us. A weakness of the present work that is imposed by our selection of EUV spectroheliograms for study, is that only one emission line has been used to probe the low temperature gas, whereas Withbroe used averaged values for several lines. Details of the upper

chromospheric Q(T) will be important for a full understanding of processes that take place at loop footpoints, and this is an important temperature range to explore. In the following discussions, we will not emphasize the upper chromospheric distribution of Q(T) observed here.

IV. DETERMINATION OF DISTRIBUTION OF T_{max}

One aim of an emission measure analysis is specification of the physical parameters that characterize the ensemble of stable loops which compose an unresolved active region. This approach requires that models for individual loops be employed that incorporate the relevant factors of distributions of non-thermal heating and plasma flow (if any) along a loop, the loop's geometry, and the heat loss rate at its footpoints. A wide range of analytic loop models have been devised under various reasonable simplifying assumptions about these factors, and they have all yielded scaling laws of the form $T_m \propto (p_o L)^{\beta}$. Vesecky, Antiochos and Underwood (1979) have compared numerical loop models with the analytical scaling laws, and found them to be reasonably useful and reliable, within their range of applicability.

Our intent is to try to develop a method by which distributions within active regions of one or more of the simple scaling parameters might be derived from an emission measure analysis. Levine and Pye undertook to do this with an elegant analytic model, but found they could not solve Q(T) for a distribution function. Like them we were not able to achieve a solution with the one analytic model we tried, but found that simple numerical models can be used.

a. Fitting to an Analytic Model

Emslie and Machado (1979) obtained semi-empirical loop models which are distinguished by two parameters, α and f, that specify the heating function's dependence on density ($E_H \sim n^{\alpha}$) and the ratio of conductive flux to radiative loss rate at the base ($f = E_{CO}/n_o^2 P(T)$). They chose $T_o = 10^4$ K at the base; together with α and f this gives the spatial temperature distribution. Finally, the emission measure q(T) is scaled by the base density n_o:

$$q(T;\ n_o,\ \alpha,\ f) = n_o\ \phi\ (T;\alpha,f) \tag{5}$$

where ϕ is a function given by the temperature distribution.

We suppose that the active regions studied by us are composed of plasma loops whose structure may be approximated by such models, and that all loops are heated by the same process and have the same α. Within an active region the distributions of base density and ratio f are such that

$$Q(T) = \sum_{n_o} \sum_{f}\ q(T;\ n_o,\ \alpha,\ f)\ w(n_o,f) \tag{6}$$

where α is fixed and w is a distribution function to be determined. We have no evidence for the form of w; it may be satisfactory to write

$$w(n_o,\ f) = w_n\ (n_o)\ w_f(f) \tag{7}$$

so that

$$Q(T) = \sum_{f} w_f(f) \left\{ \sum_{n_o'} q\ (T;\ n_o^1,\ \alpha,\ f)\ w_n\ (n_o^1) \right\} . \tag{8}$$

But, referring to equation (5),

$$Q(T) = \left\{ \sum_{f} w_f(f)\ q(T;\ n_o,\ \alpha,\ f) \right\} \sum_{n_o'}\ w_n(n_o^1)\ \frac{n_o^1}{n_o} \tag{9}$$

in which the distribution of base densities merely scales the distribution Q(T). Thus, under assumption (7), the shape of the coronal lobe of Q(T) is

decided by the distribution of f.

Although it is desirable to invert equation (9) for $w_f(f)$ this is not possible since $q(T; n_o, \alpha, f)$ becomes infinite at $T_{max} = T_m$. In real loops (Veseckey, Antiochos and Underwood, 1979) q(T) is limited by physical factors to finite values at T_m. If we suppose the semi-empirical models of Emslie and Machado (1979) represent loop structure just below T_m, we can use equation (9) to make a rough estimate of the range of f that applies.

To do this we constructed q(T) using $T_o = 10^{5.2}$K, a boundary value consistent with our observations. The highest T_m are generated with $\alpha \sim 1$ (Emslie and Machado, 1979). For an observed Q(T) that peaks near log T = 6.0 and in which there is still significant material at log T = 6.3, α must be very close to 1.

When we adopt $\alpha = 1$ we find that f = 0.92 at the peak of Q(T); since Q(T) is only scaled by $w_n(n_o^1)$ we infer from its breadth that f lies mostly in the range 0.89 -- 0.94. This estimated range of f is in good agreement with Emslie and Machado (1979), even though the maximum temperatures in our models are lower than in theirs. Because we have used a higher boundary temperature of $10^{5.2}$, and thus a correspondingly greater radiative loss than they did, our determination of the same range for f implies that a relatively greater conducted flux is deposited at the lower boundary. This is accomplished, despite the lower maximum temperatures, because less conducted flux is dissipated radiatively between the loop tops and footpoints in the models we calculated.

b. Fitting to Numerical Models

In the last section we found we could not determine a distribution function by inverting equation (9) because q(T) rises without limit at T_m. To investigate how this might be done we have resorted to using numerical models in representing q(T).

We adopt a loop of constant cross-section whose emission-measure distribution is described by its length L and maximum temperature T_m,

$$q = q(T;\ L,\ T_m)$$

The observed emission measure distribution is given by

$$Q(T) = \sum_L \sum_{T_m} q(T;\ L,\ T_m)\ w\ (L, T_m), \tag{10}$$

where w is the distribution function we seek. Again we will set

$$w(L, T_m) = w_L(L) w_m(T_m), \tag{11}$$

so that

$$Q(T) = \sum_{T_m} w_m(T_m) \left\{ \sum_L q\ (T;\ L,\ T_m)\ w_L(L) \right\} . \tag{12}$$

We suppose that a separate analysis of magnetic fields in the active regions could in principle provide an insight into the character of the distribution functions $w_L(L)$. With this information and with a model for $q\ (T;\ L,\ T_m)$ we can in principle solve equation (12) for $w_m(T_m)$. Because we do not have $w_L(L)$, even in principle, we assumed it, and with adopted models for q(T) attempted to invert the equation. The matrix is extremely ill-conditioned, and we could not achieve a direct solution; instead we have resorted to trial-and-error estimation, a method that gives satisfactory results for $w_m\ (T_m)$. In experimenting with loop models we found, however, that for some q(T)-models no complete solution was possible at all, even by this method.

Numerical models were used which were adopted from approximate polynomial fits to the temperature and electron density distributions derived by Vesecky, Antiochos and Underwood (1979). With the adopted distributions for $T(\ell)$ and $N_e(\ell)$ we constructed $q\ (T;\ L,\ T_m)$ and calculated, from equation (12), solutions $w_m\ (T_m)$ using Q(T)-data in the temperature range $5.6 < \log T < 6.5$. The calculations were restricted to this range of log T because of the uncertainty of Q(T) at $\log T < 5.5$ (discussed above). Further, our schematic numerical loop models are highly simplified and are not expected to yield a reasonable $q\ (T)$ near chromospheric temperatures. They are not necessarily in energy equilibrium everywhere, but will suffice to demonstrate results that can be obtained by inverting equation (12)

From polynomial fits to the models of Vesecky, Antiochos and Underwood (1979) we derive approximate distributions of the form

$$\log\ (N_e/N_{e,max}) = -D \log\ (\ell/L) \tag{13}$$

$$\log\ (T/T_o) = B \log \ell + C\ (\log \ell)^2 \tag{14}$$

The loops must obey a scaling law of the form $T_m = f\ (p_{oo},L)$, where $p_{oo} = p_o k = N_{e,max}\ k\ T_m$. We used the relationship developed by Craig, McClymont and Underwood (1978):

$$T_m = 3 \times 10^3\ (p_{oo}L)^{4/13}. \tag{15}$$

Whether scaling laws of this sort are valid for stable loops must still be determined (Antiochos, 1979). A numerical loop model is then specified by adopting values for B, C, D; selection of L and T_m then defines $N_{e,max}$ and T_o.

Finally, the loop's emission measure distribution is (A = area):

$$\frac{1}{A}\ q\ (T;\ L,\ T_m) = N_e^2\ \left(\frac{dT}{d\ell}\right)^{-1}. \tag{16}$$

In our calculations we fixed D = 0.36. Three sets of $q\ (T;\ L,\ T_m)$ were used in attempting solution of equation (12) for $w_m(T_m)$. In all calculations the ranges of L and T_m were $5.6 < \log T_m < 6.5$ and $9 < \log L < 10.3$. Since equation (15) requires that p_{oo} will vary greatly across this range of T_m and L, the models are not strictly compatable with the value $p_o = p_{oo}/k = 10^{16}$ K cm^{-3} used in deriving the observed Q(T). Some of the loop models from each set are shown in Figure 3.

In the model distribution of $q\ (T;\ L,\ T_m)$ the curves for a given T_m are identical in shape, and are distinguished from one another by L. For this reason, the bracketed quantity in equation (12) will always have the same T_m - dependence, independent of the choice of $w_L(L)$. This, together with the inconsistency in p_o, is a weakness of the present numerical models that can be overcome by more realistic modelling. The weighting function $w_L(L)$ that was used by us is given in Table IV.

The models shown in Figure 3 were used in equation (12) to solve for the weighting function $w_m(T)$ on 0214 UT June 8; results are shown in Figure 4. No solution for $w_m(T_m)$ is possible at the lowest T_m when models N1 and N2 are used, only loops with a very steep rise of q(T) at the loop tops (model N3) suffice to give a solution for the weighting function at the lowest T_m. The shape of the $w_m(T_m)$-distribution is essentially independent of the parameters B and C which specify the numerical models studied here, and is only scaled by the adopted values of $w_L(L)$.

Finally, we obtained distributions of the weighting function $w_m(T_m)$, using loop model N3 and the weighting function $w_L(L)$ from Table IV , for all

TABLE IV

ASSUMED WEIGHTING FUNCTION $w_L(L)$

log L	$w_L(L)$
9	1.
9.33	5.
9.66	10.
10.	5.
10.33	1.

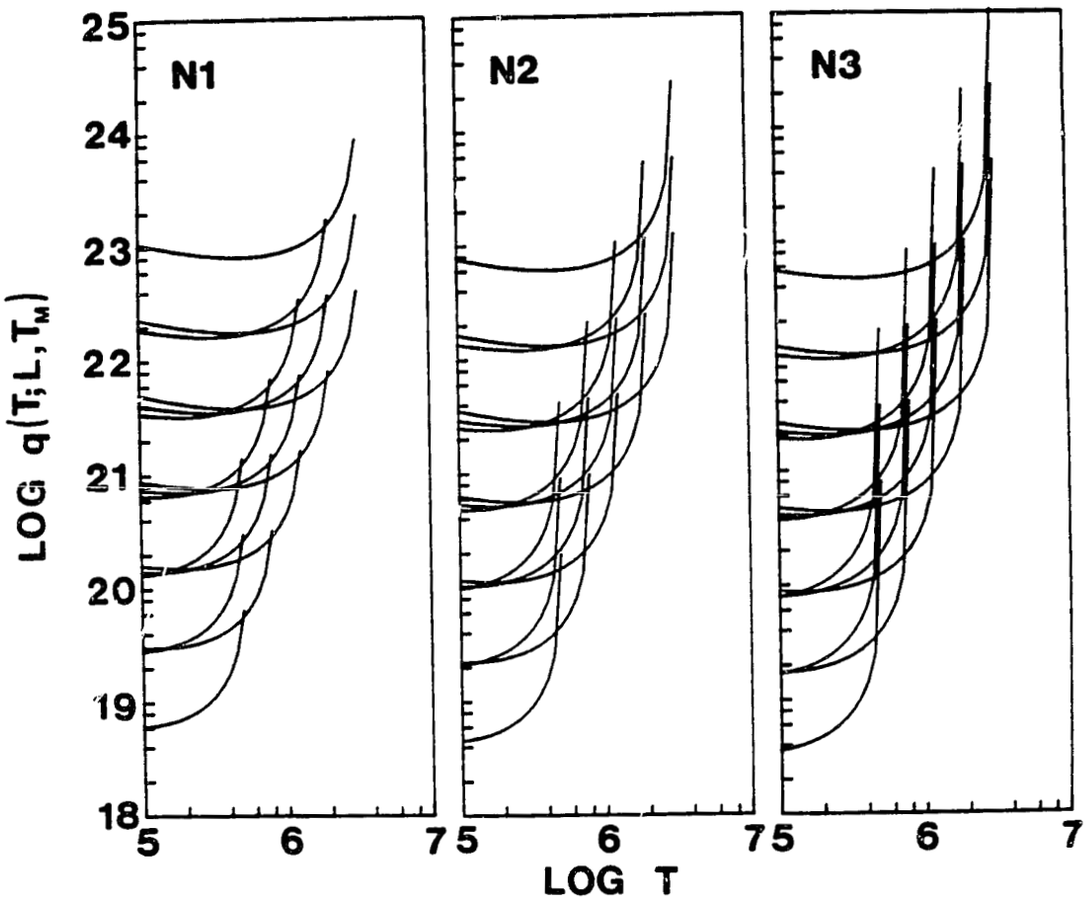

Figure 3. Emission Measure Distributions for Numerical Loop Models That Were Used To Solve Equation (12) for the Weighting Function $w_m(T_m)$. Values of B and C used in equation (14) are: Model N1, B = 0.9, C = -0.042, Model N2, B = 0.82, C = -0.040; Model N3, B = 0.705, C = -0.035. The values of log T_m are: 5.7, 5.9, 6.1, 6.3, and 6.5. Three models are shown for each T_m, corresponding to Log L values of 9.0 (upper), 9.67 (middle), and 10.33 (the lowest of three curves).

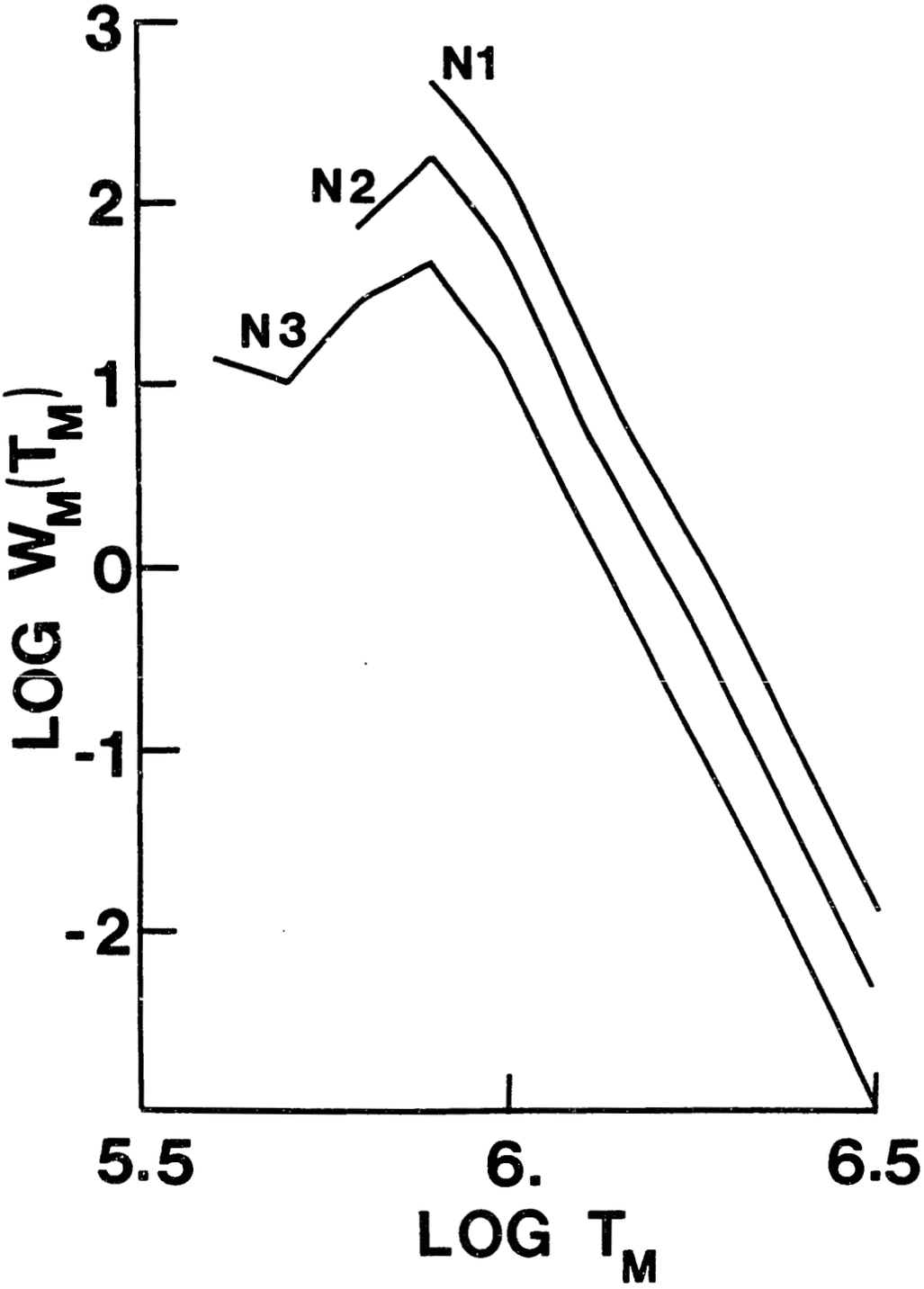

Figure 4. Solutions for the Weighting Function w_m (T_m) for the Different Loop Models. The curves for models N1 and N2 are terminated at values of log T_m below which no solution is possible.

the data. The resulting weighting functions are shown in Figure 5. The stability of these solutions against errors in observed fluxes was tested with the Q(T) -distributions that had been calculated from randomly disturbed input data (Section III). Standard deviations of solutions for w_m (T_m) obtained from data perturbed by up to 10% are listed in Table III, and indicate that the weighting functions are probably correct as to order of magnitude.

These results indicate that in compact, quiescent active regions like those studied here, unresolved plasma loops tend to prefer maximum temperatures at or below 10^6 K. Individual, resolved loops that were examined by Rosner, Tucker and Vaiana (1978) and by Emslie and Machado (1979) tend to have maximum temperatures in the vicinity of 2.5×10^6K, somewhat higher than we determined for these unresolved regions.

Differences in the temperature at which the peak of Q(T) is found may reflect the inclusion by us of fluxes derived from X-ray images, or it may reflect a real difference between large and small structures on the sun. At issue, however, is whether a useful method can be found for determining the distribution of loop properties in an active region from its integrated emission measure distribution. The present method indicates that the distribution of maximum temperatures T_m looks a great deal like the coronal lobe of Q(T).

V. SUMMARY

We have attempted to determine, from a solar active region's integrated emission measure distribution, something about the properties of the individual loops that comprise it. The present work sets some limits on such an

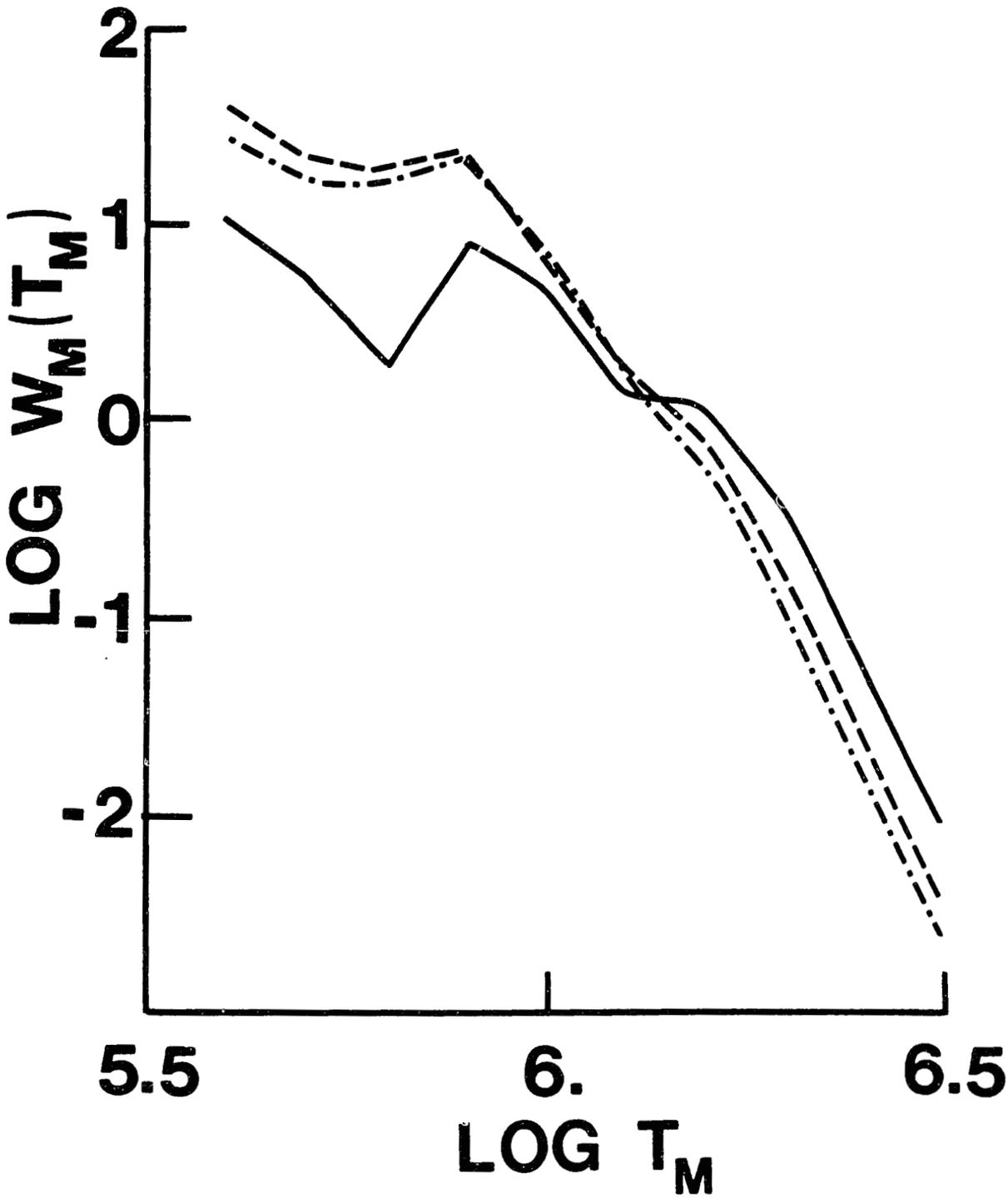

Figure 5(a). Weighting Functions w_m (T_m) for all Observed Data. Region 12364 at 1536 UT on 30 May 1973 (solid curve) and at 1946 UT on 31 May 1973 (dashed curve). Region 12375 at 2029 UT on 6 June 1973 (dot-dash curve).

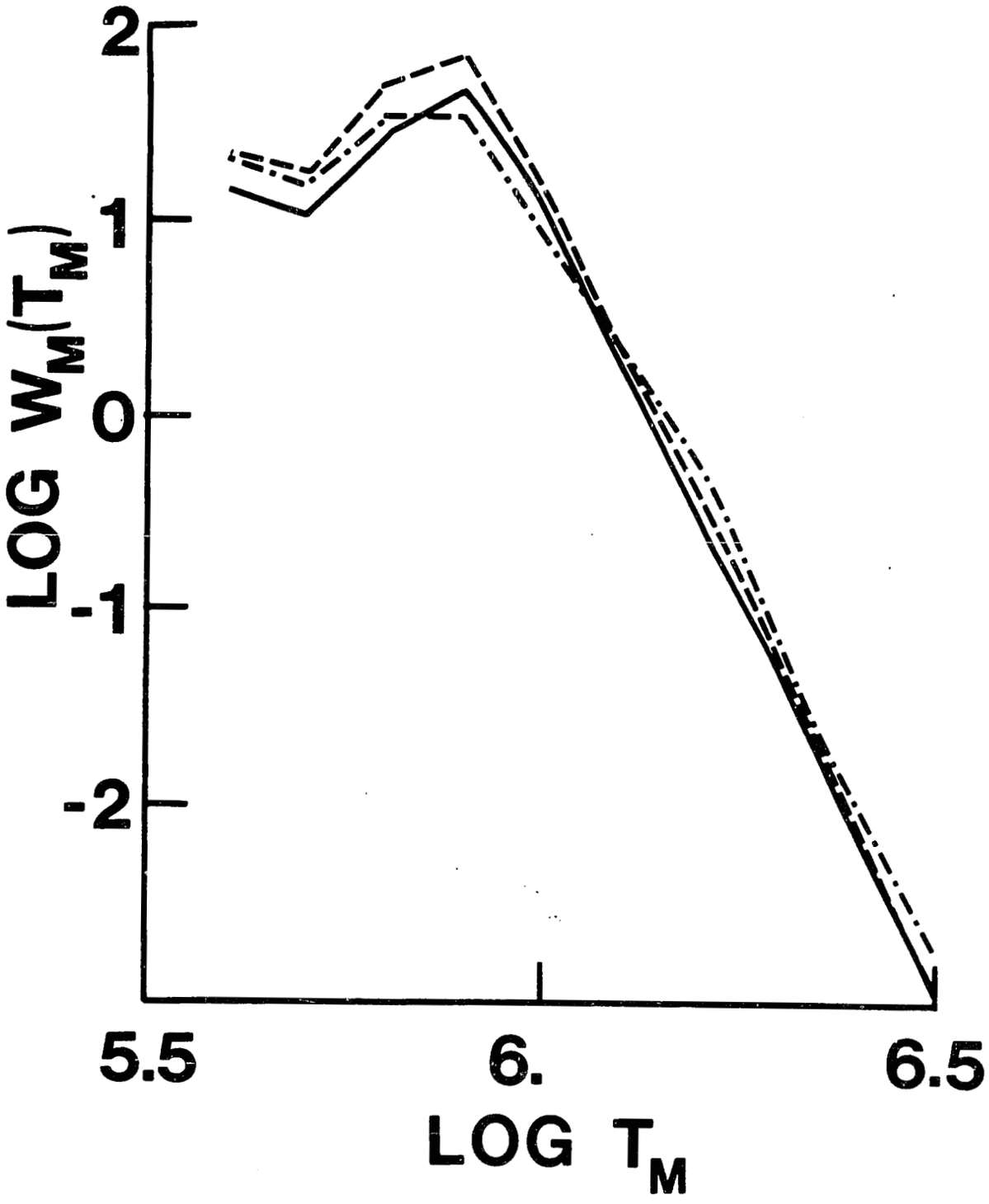

Figure 5(b). Weighting Functions w_m (T_m) for all Observed Data. Region 12378. See legend for Figure 2c for identification of curves.

approach.

Our principal result is that the Q(T) observed by us can be represented over the full range $5.6 < \log T_m < 6.5$ by the superposition of simple loop models, if the models incorporate a substantial rise in their individual q(T) near the maximum temperature T_m. This in turn suggests that the unresolved loops may have substantial area ratios Γ (Vesecky, Antiochos and Underwood, 1979), since it is this ratio that fixes the extent of the rise in q(T). Since the bulk of the emission measure then is contributed from the loop tops, the distribution of maximum temperatures has approximately the same shape as does the integrated Q(T).

REFERENCES

Antiochos, S. K.: 1979, Astrophys. J. Lett. 232, L125.

Craig, J. D., McClymond, A. N., and Underwood, J. H.: 1978, Astron. and Astrophys. 70, 1.

Dupree, A. K.: 1972, Astrophys. J. 178, 527.

Dupree, A. K., Huber, M. C. E., Noyes, R. W., Parkinson, W. H., Reeves, E. M. and Withbroe, G. L.: 1973, Astrophys. J. 182, 321.

Emslie, A. G. and Machado, M. F.: 1979, Ctr. for Astrophysics Preprint No. 1034.

Foukal, P.: 1976, Solar Phys. 43, 327.

Habbal, S. R. and Rosner, R.: 1979, Astrophys. J. 234, 1113.

Levine, R. H. and Pye, J. P.: 1979, Ctr. for Astrophysics Preprint No. 1202.

Nicolas, K. R., Bartoe, J.-D. F., Brueckner, G. E. and VanHoosier, M. E.: 1979, Astrophys. J. 233, 741.

Pye, J. P., Evans, K. D., Hutcheon, R. J., Gerassimenko, M., Davis, J. M., Krieger, A. S. and Veecky, J. F.: 1978, Astron. and Astrophys. 65, 123.

Raymond, J. C. and Dupree, A. K.: 1978, Astrophys. J. 222, 379.

Reeves, E. M., Huber, M. C. E. and Timothy, J. G.: 1977, Appl. Opt. 16, 837.

Reeves, E. M., Timothy, J. G., Huber, M. C. E. and Withbroe, G. L.: 1977, Appl. Opt. 16, 849.

Rosner, R., Tucker, W. H. and Vaiana, G. S.: 1978, Astrophys. J. 220, 643.

Underwood, J. H. and McKenzie, D. L.: 1977, Solar Phys. 53, 417.

Underwood, J. H., Milligan, J. E., deLoach, A. C. and Hoover, R. B.: 1977, Appl. Opt. 16, 858.

Vaiana, G. S., Krieger, A. S., Timothy, A. F. and Zombeck, M. V.: 1976, Astr. Space Sci. 39, 75.

Vernazza, J. E. and Reeves, E. M.: 1978, Astrophys. J. Suppl. 37, 485.

Vernazza, J. E. and Raymond, J. C.: 1979, Astrophys. J. Lett. 228, L89.

Vesecky, J. F., Antiochos, S. K. and Underwood, J. H.: 1979, Astrophys. J. 233, 987.

Withbroe, G. L.: 1975, Solar Phys. 45, 301.

Withbroe, G. L.: 1977, Proceedings of the OSO-8 Workshop, Boulder.